

PbTe/CdTe Core/Shell Particles by Cation Exchange, a HR-TEM study

Karel Lambert, Bram De Geyter, Iwan Moreels, and Zeger Hens*

Physics and Chemistry of Nanostructures, Ghent University, Krijgslaan 281–S12, B-9000 Ghent, Belgium

Received October 28, 2008

Revised Manuscript Received January 28, 2009

Core/shell quantum dots are heterogeneous nanoparticles composed of an inorganic core enveloped by at least one inorganic shell of a second material. These structures have attracted increasing attention over the past decade, especially because of their enhanced photoluminescence properties^{1–4} and the possibility to create spatially separated excitons by means of a staggered core/shell band alignment.^{5,6} Synthesis of core/shell structures involves epitaxial growth of a second semiconductor onto seed particles, in either a single-step^{7,8} or multistep reaction.⁹ An alternative mechanism to form this type of heterogeneous nanocrystals exploits cation exchange, which has been demonstrated in various materials such as CdS–PbS,¹⁰ CdS–Ag₂S,^{11,12} and CdSe–ZnSe.¹³ More recently, the formation of PbS/CdS and PbSe/CdSe core/shell QDs by cation exchange has been demonstrated,¹⁴ which avoids the problems these materials have with luminescence stability and oxidation. Although attractive because of its simplicity, the cation exchange method has its limitations. For some systems, there is a size limit below which the geometry of the particles is not maintained,¹¹ or diffusion may alter the composition of the core.¹³

In this communication, we take the PbS/CdS and PbSe/CdSe core/shell formation by cation exchange as reported by

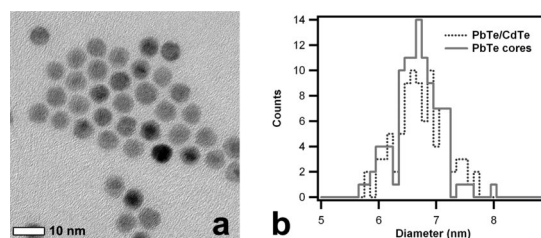


Figure 1. (a) High-contrast TEM image of PbTe/CdTe QDs, showing a distinct core/shell structure in some of the particles. (b) Comparison of the size distribution of the PbTe cores and PbTe/CdTe core/shell particles.

Pietryga and co-workers as a starting point.¹⁴ First, we show that the method can be extended to PbTe/CdTe. Second, we demonstrate that the combination of the PbTe rocksalt structure and the CdTe zincblende structure allows for the direct observation of the core and the shell with high-resolution transmission electron microscopy (HR-TEM). This enables a direct visualization of the crystallographic properties of the PbTe/CdTe QDs and an evaluation of the cation exchange reaction. We observe a seamless match between the PbTe and CdTe crystal lattices and find that the formation of {111} terminated PbTe cores is favored. This intrinsic anisotropy of the exchange process leads to a strong increase in the heterogeneity of the cores formed, not only in terms of core size and shell thickness but also at the level of shape and position of the core. Clearly, this is an important drawback of this apparently straightforward core/shell synthesis technique.

PbTe core particles were synthesized according to literature methods.¹⁵ Cationic exchange of Pb by Cd was achieved by adding an excess of Cd oleate dissolved in ODE to the QD suspension in toluene, heated to 100 °C (see the Supporting Information). Using PbTe cores with a mean diameter d of 6.6 nm and a size dispersion σ of 6.6%, HR-TEM images show that this results in PbTe/CdTe particles with $d = 6.7$ nm and $\sigma = 6.4\%$ (Figure 1). Hence, cationic exchange changes neither the mean diameter nor the size dispersion of the particles. As with the published high contrast images of PbSe/CdSe QDs,¹⁴ a distinct core/shell structure is visible in some of the particles. Elemental analysis on ensembles of QDs with TEM-based energy-dispersive X-ray analysis (TEM-EDS) shows the presence of Pb, Cd and Te after cationic exchange (see the Supporting Information). Moreover, a STEM-EDS line scan through the center of a single particle demonstrates that Cd and Te are present over the entire width of the particle, whereas Pb is limited to a narrow region near the particle center (Figure 2). This demonstrates that individual particles consist of a PbTe core and a CdTe shell. The position of the Pb peak indicates an eccentric core.

* Corresponding author. E-mail: zeger.hens@ughent.be.

- (1) Hines, M. A.; Guyot-Sionnest, P. *J. Phys. Chem.* **1996**, *100*, 468–471.
- (2) Dabbousi, B. O.; Rodrigues-Viejo, J.; Mikulec, F. V.; Heine, J. R.; Mattoussi, H.; Ober, R.; Jensen, K. F.; Bawendi, M. G. *J. Phys. Chem. B* **1997**, *101*, 9463–9475.
- (3) Peng, X. G.; Schlamp, M. C.; Kadavanich, A. V.; Alivisatos, A. P. *J. Am. Chem. Soc.* **1997**, *119*, 7019–7029.
- (4) Aharoni, A.; Mokari, T.; Popov, I.; Banin, U. *J. Am. Chem. Soc.* **2006**, *128*, 257–264.
- (5) Battaglia, D.; Blackman, B.; Peng, X. *J. Am. Chem. Soc.* **2005**, *127*, 10889–10897.
- (6) Sapra, S.; Mayilo, S.; Klar, T. A.; Rogach, A. L.; Feldmann, J. *Adv. Mater.* **2007**, *19*, 568.
- (7) Mekis, I.; Talapin, D. V.; Kornowski, A.; Haase, M.; Weller, H. *J. Phys. Chem. B* **2003**, *107*, 7454–7462.
- (8) Xu, S.; Ziegler, J.; Nann, T. *J. Mater. Chem.* **2008**, *18*, 2653–2656.
- (9) Li, J. J.; Wang, Y. A.; Guo, W. Z.; Keay, J. C.; Mishima, T. D.; Johnson, M. B.; Peng, X. G. *J. Am. Chem. Soc.* **2003**, *125*, 12567–12575.
- (10) Zhou, H. S.; Honma, I.; Komiyama, H.; Haus, J. W. *J. Phys. Chem.* **1993**, *97*, 895–901.
- (11) Son, D. H.; Hughes, S. M.; Yin, Y.; Alivisatos, A. P. *Science* **2004**, *306*, 1009–1012.
- (12) Robinson, R. D.; Stadler, B.; Demchenko, D. O.; Erdonmez, C. K.; Wang, L.-W.; Alivisatos, A. P. *Science* **2007**, *317*, 355–358.
- (13) Zhong, X.; Feng, Y.; Zhang, Y.; Gu, Z.; Zou, L. *Nanotechnology* **2007**, *18*, 385606.
- (14) Pietryga, J. M.; Werder, D. J.; Williams, D. J.; Casson, J. L.; Schaller, R. D.; Klimov, V. I.; Hollingsworth, J. A. *J. Am. Chem. Soc.* **2008**, *130*, 4879–4885.

- (15) Murphy, J. E.; Beard, M. C.; Norman, A. G.; Ahrenkiel, S. P.; Johnson, J. C.; Yu, P.; Micic, O. I.; Ellingson, R. J.; Nozik, A. J. *J. Am. Chem. Soc.* **2006**, *128*, 3241–3247.

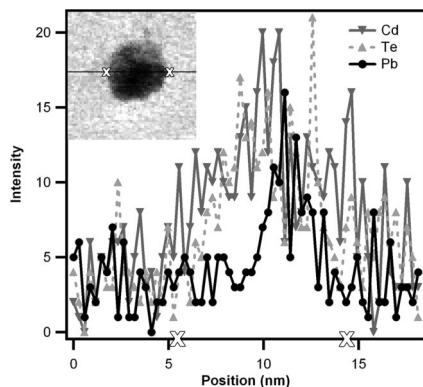


Figure 2. STEM-EDS line scan along a single PbTe/CdTe core-shell particle (see inset), showing the presence of Pb only in the particle center. The particle edges are marked with X.

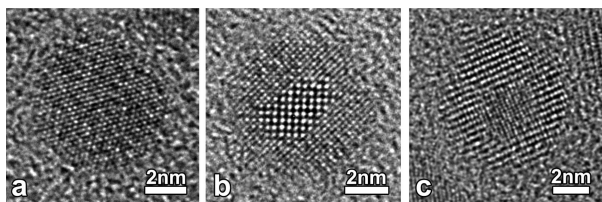


Figure 3. HR-TEM images of PbTe/CdTe core-shell particles in the (a) $\langle 111 \rangle$, (b) $\langle 100 \rangle$, and (c) $\langle 211 \rangle$ direction. A core-shell structure is observed only in the $\langle 100 \rangle$ and $\langle 211 \rangle$ directions.

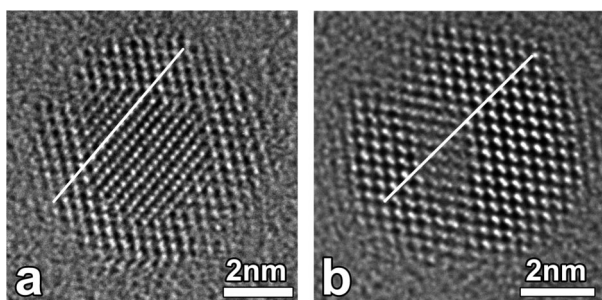


Figure 4. HR-TEM images of PbTe/CdTe core-shell particles in the $\langle 110 \rangle$ direction. In some particles, the lattice at one end of the core is shifted with respect to the lattice at the other end.

Both PbTe and CdTe have a cubic crystal structure with almost no lattice mismatch (rocksalt with a lattice constant of 0.6462 nm and zincblende with 0.6480 nm, respectively¹⁶). Yet, Figures 3 and 4 show that resolved core-shell lattice images can be obtained in HR-TEM for specific orientations of the particles. The reason is that the appearance of the crystal lattice in HR-TEM not only depends on the crystal orientation but also on the defocus. Therefore, the same crystal plane may yield a different lattice image for both materials.

Along the $\langle 111 \rangle$ direction, the lattice image of both PbTe and CdTe shows a hexagonal pattern with an almost identical lattice constant of 0.280 and 0.281 nm (see the Supporting Information). Figure 3a gives an example of a PbTe/CdTe core-shell QD that exhibits this pattern. It appears as a simple, uniform particle with a continuously resolved lattice and no indication of any core-shell structure. This result is typical for all particles viewed along the $\langle 111 \rangle$ direction. It shows

that core and shell have their $\langle 111 \rangle$ axis pointing in the same direction, with a coherent alignment of the $\{111\}$ planes. When viewed along the $\langle 100 \rangle$ direction, PbTe and CdTe may yield two types of lattice images with square symmetry (see the Supporting Information). The first has a lattice constant of 0.323 nm (PbTe) or 0.324 nm (CdTe), the second is tilted by 45° and has a lattice constant of 0.229 nm for both PbTe and CdTe. Figure 3b represents an image where a core is observed that exhibits a 0.321 nm square pattern and a shell that exhibits a 0.234 nm square pattern. Obviously, we associate the former with the PbTe core and the latter with the CdTe shell. Both patterns are tilted by 45° and match seamlessly, but the interface between them is not clear-cut. Again, this image demonstrates that core and shell have their $\langle 100 \rangle$ axis pointing in the same direction, with a coherent alignment of the $\{100\}$ planes. Along the $\langle 211 \rangle$ direction, PbTe and CdTe yield a rectangular lattice image with 0.229/0.194 nm and 0.389/0.229 nm unit cells, respectively (see the Supporting Information). Figure 3c shows an image where both lattice images can be seen. As in the $\langle 100 \rangle$ direction, both lattices match seamlessly, but there is no distinct interface in between.

Viewed along the $\langle 110 \rangle$ direction, PbTe yields two possible rectangular lattice images, a first with a 0.646/0.457 nm and a second with a 0.323/0.229 nm unit cell, respectively. For CdTe, we find only a rectangular pattern with a 0.648/0.459 nm unit cell (see the Supporting Information). Figure 4a gives an example of a PbTe/CdTe core shell particle featuring a core with the 0.323/0.229 nm unit cell and a shell with the 0.648/0.459 nm unit cell. Again, we simultaneously observe identical crystal planes of both core and shell, and these planes are mutually aligned. Moreover, the core-shell structure viewed along the $\langle 110 \rangle$ direction shows well-defined crystallographic boundaries between the core and the shell. These mainly follow the $\langle 111 \rangle$ directions, and sometimes the $\langle 100 \rangle$ directions.

The most extensively studied PbTe/CdTe interface in literature is probably that between the PbTe and CdTe $\{110\}$ planes, as found with self-assembled PbTe quantum dots in a CdTe matrix.^{17,18} In this case, a coherent interface is observed, which was attributed to the continuation of the Te sublattice between both materials. Our results point toward a similar coherence between the PbTe and the CdTe lattice, although the images along $\langle 110 \rangle$ indicate that interfacing is mainly along the $\{111\}$ planes. The dominance of one specific interface, and the occurrence of nonspherical and eccentric cores (see further), is not in line with an isotropic exchange process. The observed anisotropy may be imposed by thermodynamics (interfacial tension) or by the exchange mechanism. Ab initio calculations of interfacial energies for PbTe/CdTe interfaces show values of around 0.20 J/m² for the $\{111\}$, $\{110\}$, and $\{100\}$ facets. At thermodynamic equilibrium, this should result in a rhombocuboctahedral core shape.¹⁸ Although the presence of edges and vertices can considerably influence the shape of

(16) Koike, K.; Honden, T.; Makabe, I.; Yan, F. P.; Yano, M. *J. Cryst. Growth* **2003**, 257, 212–217.

(17) Leitsmann, R.; Ramos, L. E.; Bechstedt, F.; Groiss, H.; Schäffler, F.; Heiss, W.; Koike, K.; Harada, H.; Yano, M. *New J. Phys.* **2006**, 8, 317.

(18) Leitsmann, R.; Ramos, L. E.; Bechstedt, F. *Phys. Rev. B* **2006**, 74, 085309.

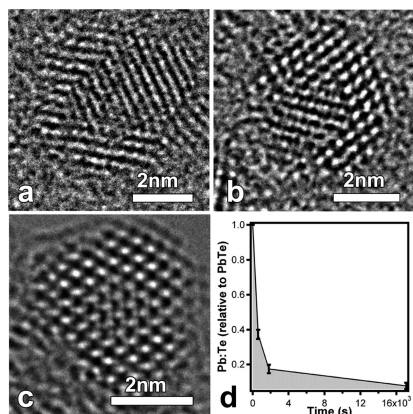


Figure 5. HR-TEM images of PbTe/CdTe core-shell particles in the $\langle 110 \rangle$ direction after different exchange reaction times: (a) 10 min (63% exchanged), (b) 30 min (83% exchanged), and (c) 4 h 45 min (92% exchanged). (d) The exchange of Pb by Cd was determined by TEM-EDS on ensembles of nanoparticles.

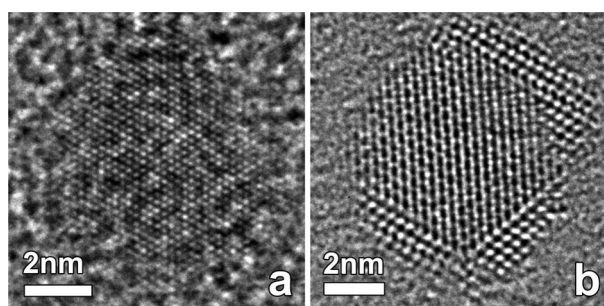


Figure 6. HR-TEM images of PbSe/CdSe core-shell particles in the (a) $\langle 111 \rangle$ and (b) $\langle 110 \rangle$ directions.

small cores,^{18,19} the dominance of $\{111\}$ interfaces—in contrast with self-assembled PbTe/CdTe QDs—suggests that the core shape resulting from cationic exchange is not determined by thermodynamics, but rather by an anisotropic growth mechanism. We verified this conclusion by imaging core-shell particles after different reaction times (Figure 5). We always find that the core edges are almost exclusively defined by $\{111\}$ planes, regardless of the extent of the exchange as determined by TEM-EDS. The measurements also show that the exchange reaction initially proceeds fast, but slows down considerably as more of the Cd is exchanged.

As yet, the origin of the anisotropy is unclear. However, it is not limited to the PbTe/CdTe system. Figure 6 shows lattice images of PbSe/CdSe QDs made with a similar cationic exchange procedure¹⁴ (see the Supporting Information). As compared to PbTe/CdTe, the crystal structure of the core and the shell are the same, with a slightly larger lattice mismatch of around 1% in the case of PbSe/CdSe.¹⁴ Figure 6a shows a PbSe/CdSe particle viewed along the $\langle 111 \rangle$ direction. As with PbTe/CdTe, no core-shell structure is observed. Along $\langle 110 \rangle$, however, we clearly see a distinct core with mainly $\{111\}$ and some $\{100\}$ interfaces, similar to what we found with PbTe/CdTe. This indicates that the

anisotropy is related to the crystal structure of the core and/or the shell material.

The strong anisotropy of the exchange reaction has implications for the monodispersity of the PbTe cores. From a statistical analysis on 46 of the 6.7 nm core-shell particles imaged by HR-TEM, we find that the remaining PbTe cores have an average equivalent circle diameter of 3.5 nm. The initial size dispersion of 6.6% has increased to 25%. Moreover, the average size hides a variety of positions and aspect ratios. This runs from almost spherical cores to cores with an aspect ratio of 1:2.2 and from cores that are at the center of the quantum dot to cores that are completely at one side of the final structure. We conclude that cationic exchange leads to a strong increase of sample heterogeneity. Another issue with the exchange reaction is the introduction of defects in the crystal structure. Whereas HR-TEM images of the original PbTe particles do not exhibit lattice defects, evidence of distortions was found in many of the core-shell particles. In Figure 4, we present two QDs viewed along the $\langle 110 \rangle$ direction. The first is the more conventional situation, where we find a seamless continuation of the lattice image at either side of the core (indicated by the line in Figure 4a). In the second, we see that the lattice at the left of the core is shifted by a quarter of a unit cell in the $\langle 001 \rangle$ direction relative to that at the right of the core (indicated by the line in Figure 4b). A possible explanation is that at either side of the core, a different sublattice is continued. Clearly, such a shift induces considerable strain in the shell lattice.

In summary, we have grown a CdTe shell around PbTe core particles using cationic exchange and evaluated the resulting core-shell particles using TEM-based techniques. The formation of a CdTe shell is demonstrated directly by STEM-EDS and HR-TEM imaging. Core and shell have the same crystallographic orientation with a seamless match of their crystal lattices and mainly $\{111\}$ interfaces. The latter is indicative of an anisotropic exchange mechanism. It results in a strong increase of the heterogeneity of the nanocrystals, in terms of the geometry (core size and shape, position of the core in the core-shell particle), but also in terms of crystallography of the core-shell structure. Similar results were obtained for PbSe/CdSe particles. We conclude that in the case of lead chalcogenides, cationic exchange is a straightforward technique to form lead chalcogenide/cadmium chalcogenide core-shell particles, yet involving an important drawback in terms of a considerable increase in the sample heterogeneity.

Acknowledgment. The authors acknowledge the Belgian Science Policy (IAP 6/10—photonics@be) and Ghent University for a research grant. I.M. thanks the Institute for the Promotion of Innovation through Science and Technology in Flanders (IWT-Vlaanderen) for a scholarship.

Supporting Information Available: Details about QD synthesis, extra HR-TEM pictures of PbTe/CdTe and PbSe/CdSe, and HR-TEM simulations for bulk PbTe and CdTe (PDF). This material is available free of charge via the Internet at <http://pubs.acs.org>.

(19) Groiss, H.; Kaufmann, E.; Springholz, G.; Schwarzi, T.; Hesser, G.; Schäffler, F.; Heiss, W.; Koike, K.; Itakura, T.; Hotei, T.; Yano, M.; Wojtowicz, T. *Appl. Phys. Lett.* **2007**, *91*, 222106.